

Stomatal responses in grapevine become increasingly more tolerant to low water potentials throughout the growing season

Jose Carlos Herrera^{1*} , Alberto Calderan^{2,3}, Gregory A. Gambetta⁴, Enrico Peterlunger², Astrid Forneck¹, Paolo Sivilotti², Herve Cochard⁵ and Uri Hochberg^{6*}

¹Institute of Viticulture and Pomology, Department of Crop Sciences, University of Natural Resources and Life Sciences, Vienna (BOKU), Tulln, Austria,

²Department of Agricultural, Food, Environmental and Animal Sciences, University of Udine, Udine, Italy,

³Department of Life Sciences, University of Trieste, Trieste, Italy,

⁴EGFV, Bordeaux-Sciences Agro, INRAE, Université de Bordeaux, ISVV, Villenave d'Ornon, France,

⁵INRAE, PIAF, Université Clermont-Auvergne, Clermont-Ferrand 63000, France, and

⁶Institute of Soil, Water and Environmental Sciences, Volcani Center, Agricultural Research Organization, Bet-Dagan, Israel

Received 6 June 2021; revised 8 November 2021; accepted 15 November 2021; published online 19 November 2021.

*For correspondence (e-mails jose.herrera@boku.ac.at; hochberg@volcani.agri.gov.il).

SUMMARY

The leaf of a deciduous species completes its life cycle in a few months. During leaf maturation, osmolyte accumulation leads to a significant reduction of the turgor loss point (Ψ_{TLP}), a known marker for stomatal closure. Here we exposed two grapevine cultivars to drought at three different times during the growing season to explore if the seasonal decrease in leaf Ψ_{TLP} influences the stomatal response to drought. The results showed a significant seasonal shift in the response of stomatal conductance to stem water potential ($g_s \sim \Psi_{stem}$), demonstrating that grapevines become increasingly tolerant to low Ψ_{stem} as the season progresses in coordination with the decrease in Ψ_{TLP} . We also used the SurEau hydraulic model to demonstrate a direct link between osmotic adjustment and the plasticity of $g_s \sim \Psi_{stem}$. To understand the possible advantages of $g_s \sim \Psi_{stem}$ plasticity, we incorporated a seasonally dynamic leaf osmotic potential into the model that simulated stomatal conductance under several water availabilities and climatic scenarios. The model demonstrated that a seasonally dynamic stomatal closure threshold results in trade-offs: it reduces the time to turgor loss under sustained long-term drought, but increases overall gas exchange particularly under seasonal shifts in temperature and stochastic water availability. A projected hotter future is expected to lower the increase in gas exchange that plants gain from the seasonal shift in $g_s \sim \Psi_{stem}$. These findings show that accounting for dynamic stomatal regulation is critical for understanding drought tolerance.

Keywords: water stress, *Vitis vinifera*, vine hydraulics, pressure-volume curves, osmotic adjustment, drought acclimation, isohydric, anisohydric, stomatal conductance.

INTRODUCTION

Stomata are the tiny pores on the leaf surface, controlling gas exchange between the plant and the atmosphere (Darwin, 1898). Our understanding of a multitude of critical issues in plant science, (e.g. crop irrigation requirements, plant productivity, global terrestrial evapotranspiration fluxes) relies on a sound knowledge of the regulation of these tiny pores (Jasechko et al., 2013). It is well established that leaf dehydration induces hydraulic and chemical signals that lead to stomatal closure (Buckley, 2019). Therefore, stomatal conductance (g_s) response to water potential (Ψ) is considered an underlying physiological

characteristic of a species (Brown et al., 1976; O'Toole and Cruz, 1980). These curves ($g_s \sim \Psi$) are frequently reduced into a single number that represents the water potential that leads to 50% or 75% stomatal closure ($\Psi_{g_{s50}}$ or $\Psi_{g_{s25}}$, respectively; Klein, 2014) and often used to compare species for their stomata sensitivity to closure during drought (Henry et al., 2019). $\Psi_{g_{s50}}$ is a plastic trait, changing in respect to soil type (Tramontini et al., 2014), drought acclimation (Hochberg et al., 2017a), sink strength (Naor et al., 2013), CO_2 availability (Field et al., 1995; Morison, 2001), temperature (Sepúlveda and Kliewer, 1986), and nutrient availability (Radin, 1984; Radin and Ackerson, 1981).

However, despite evidence that $\Psi_{g_{s50}}$ is also seasonally plastic (introduced below), there have been no direct quantitative measurements of this plasticity. This is probably due to the difficulty in generating a $g_s \sim \Psi$ curve for a specific time of year, as it can take weeks or months to dry out a tree under natural conditions. Therefore, most evidence for the seasonal plasticity of stomatal regulation comes from indirect measurements of other variables.

Over 40 years ago, Hardie and Considine (1976) showed that when potted grapevines were deprived of irrigation until the appearance of desiccated shoot tips and leaf abscission, they had to be dried to lower predawn water potentials (Ψ_{PD}) late in the season as compared with early-season drought. At the time, these authors did not attribute their findings to the seasonal plasticity of stomatal regulation, but during the last two decades several findings supported the idea that later in the season the down-regulation of g_s would potentially occur under more negative Ψ . First, several authors indicated that mature leaves (whose proportion likely increases along the season) close their stomata under lower Ψ as compared with younger leaves (Jordan et al., 1975; Patakas et al., 1997). Mature leaves typically have higher leaf mass per area, better lignified cell walls, and more negative solute potential, allowing them to maintain transpiration while sustaining low Ψ_{stem} (Hsiao et al., 1976; Patakas and Noitsakis, 2001). In addition, the difference between midday leaf water potential (Ψ_l) and Ψ_{PD} ($\Delta\Psi$) typically increases along the season (Martorell et al., 2015; Padgett-Johnson et al., 2003; Figure 1; Figure S1). This $\Delta\Psi$ is negatively correlated with $\Psi_{g_{s50}}$ and was suggested to describe the drought strategy of plants (Franks et al., 2007). Furthermore, the $g_s \sim \Psi$ regression across several irrigation treatments tended to more negative Ψ later in the season (Naor, 2008). Perhaps the strongest evidence is that the turgor loss point (Ψ_{TLP}), which is considered a proxy for stomatal closure (Brodribb et al., 2003; Dayer et al., 2020; Farrell et al., 2017), was shown to decrease gradually as the season progresses (Alsina et al., 2007; Martorell et al., 2015). The link between Ψ_{TLP} and $g_s \sim \Psi$ has a simple mechanical explanation. The seasonal accumulation of solutes in most species allows plants to maintain turgor under lower Ψ at the end of summer (Bartlett et al., 2014). As turgor pressure has a positive mechanical link with the pore size between the guard cells (Meidner and Edwards, 1975), the late season higher solute concentration should also result in higher stomatal conductance for any given Ψ . Accordingly, the seasonal adjustment of Ψ_{TLP} (Bartlett et al., 2014) is likely to drive an equal adjustment of $g_s \sim \Psi$.

In this study, we aimed to explore the differences in $g_s \sim \Psi_{stem}$ of potted grapevines exposed to drought in the early, middle, or late stages of the growing season. Our hypothesis was that $g_s \sim \Psi_{stem}$ is plastic and changes to lower water potential in coordination with the seasonal

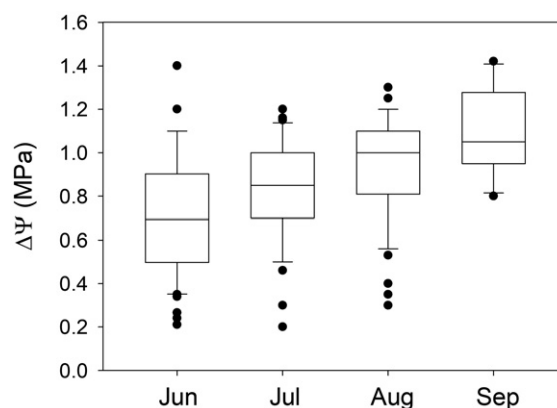


Figure 1. Hydraulic behaviour of *Vitis vinifera* in June, July, August, and September.

Box plots represent the differences between leaf midday and predawn water potential ($\Delta\Psi$) along the growing season. Data were taken from the *V. vinifera* hydraulic database (supplementary data in Hochberg et al., 2018); the predawn and midday leaf water potential dataset is presented separately in Figure S1.

modifications of the Ψ_{TLP} . In addition, we used the SurEau hydraulic model (Cocharde et al., 2021) to (i) check if osmotic adjustment alone suffices to create a significant modification in $g_s \sim \Psi_{leaf}$ and (ii) explore the advantage of a seasonal dynamic stomatal closure threshold on whole-plant water use and its regulation under drought.

RESULTS

Dehydration experiment

The dehydration experiment was designed to investigate the seasonal plasticity of $g_s \sim \Psi_{stem}$ in grapevines (*Vitis vinifera* L. cvs. Cabernet Sauvignon and Syrah). To do so, drought stress was imposed by withholding irrigation at different stages of the season (namely June, July, and September) while simultaneously measuring stomatal conductance (g_s) and stem water potential (Ψ_{stem}), as well as the leaf pressure–volume relation.

The climatic conditions during the drought stress trials recorded an average $VPD_{max} = 1.95$ kPa and average $T_{max} = 30.1^\circ\text{C}$ in June, while in July the average $VPD_{max} = 2.27$ kPa and average $T_{max} = 31.1^\circ\text{C}$. In September, the weather was slightly cooler and more humid (average $VPD_{max} = 1.76$ kPa; average $T_{max} = 27.8^\circ\text{C}$; Figure S2). It is important to state that the drought stress periods were planned to be performed under mostly sunny conditions (i.e. the decision on when to start withholding of the irrigation was made considering the weather forecast).

Budbreak occurred simultaneously in both cultivars [day of the year (DOY) 125], and by the time of the first drought stress imposition (DOY 172) the leaf area was on average 0.122 ± 0.01 m² per vine, without significant differences between Cabernet Sauvignon and Syrah. In the second

drought stress period, on DOY 199, the leaf area was increased with no significant differences between cultivars (0.145 ± 0.03 and 0.175 ± 0.04 m² per vine in Cabernet Sauvignon and Syrah, respectively). By DOY 255, during the last drought stress, the Cabernet Sauvignon leaf area (0.488 ± 0.03 m² per vine) was significantly larger than Syrah (0.340 ± 0.04 m² per vine), mainly due to a higher development of lateral shoots (Table S1).

The Ψ_{stem} measurements showed that during the earliest drought imposition (June), the minimum Ψ_{stem} was reached by both grapevine cultivars leading to $g_s < 50$ mmol m⁻² sec⁻¹ and the appearance of any wilting or leaf abscission symptoms was on average about -1.0 MPa, while it decreased to -1.3 and to -1.8 MPa in July and September, respectively (Figure 2). In Figure S3 the relative values of Ψ_{stem} (calculated as the arithmetic difference between WS and WW treatments) are presented confirming the trends towards more negative values with the season progression. For all three drought trials, g_s decreased from maximums of 200–300 mmol m⁻² sec⁻¹ before the withholding of watering (with no differences between

cultivars and times) down to <20 mmol m⁻² sec⁻¹ towards the end of each drought event (Figure 2).

Leaf pressure–volume analysis revealed that the osmotic potential at full turgor (π_{100}) and Ψ_{TLP} decreased by about 0.1 MPa per month in both cultivars. The other considered parameters, i.e. relative water content at turgor loss point (RWC_{TLP}) and bulk modulus of elasticity (ϵ), did not change significantly (Table 1). Both cultivars behaved nearly identically, with Ψ_{TLP} decreasing from -1.18 MPa in June to -1.49 MPa in September (average of both cultivars). As hypothesized, along with the gradual change in Ψ_{TLP} the stomatal response curves also shifted to lower Ψ_{stem} (Figure 3). It could be interpreted that the g_s – Ψ_{stem} curves are less steep in September than earlier in the season, possibly reflecting the effects of other hydraulic parameters that are seasonally dynamic and not considered in this study (e.g. K_{leaf} , K_{plant} , and capacitance).

To test the differences in the stomatal response to water potential throughout the season we used the model g_s – $\Psi_{\text{stem}} \times \text{Month}$ (where “Month” represents the moment of drought imposition). While the Ψ_{stem} factor was always

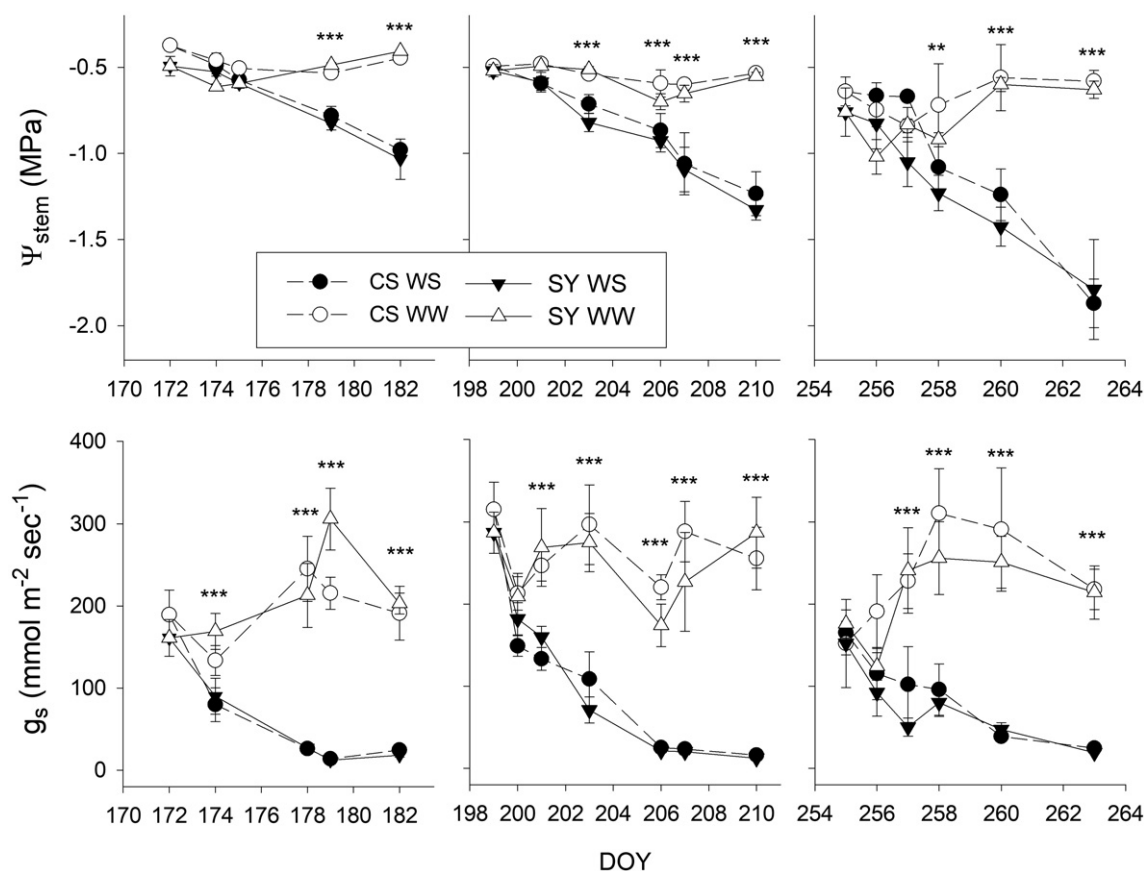
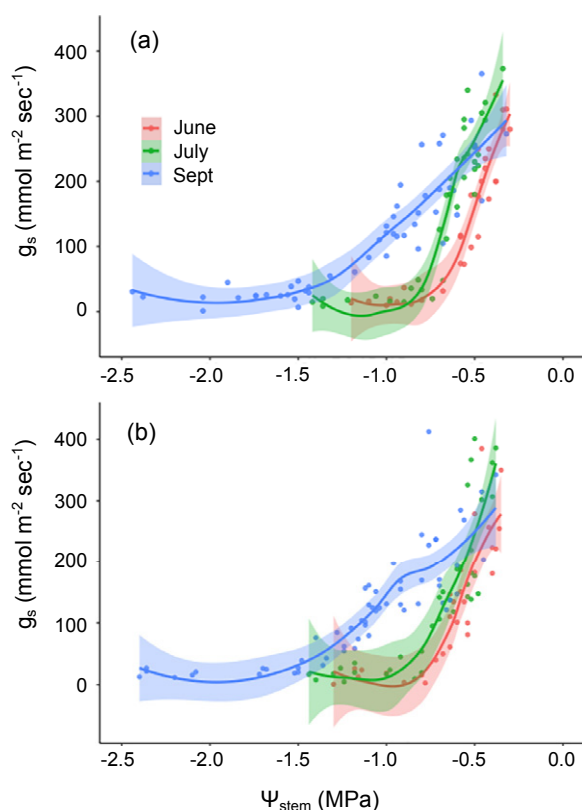


Figure 2. Midday stem water potential (Ψ_{stem}) and stomatal conductance (g_s) measured during the three different drought experiments on Cabernet Sauvignon (CS; circles) and Syrah (SY; triangles) subjected to water stress (WS; closed symbols) or well-watered controls (WW; open symbols). Values are means \pm SEM (Ψ_{stem} $n = 3$ –5; g_s $n = 6$ –10). ***, **Differences at $P < 0.001$ and 0.01, respectively, between WW and WS at a given date. No differences between CS and SY were found. DOY, day of year.

Table 1 Leaf pressure–volume curve parameters of Syrah and Cabernet Sauvignon vines in June, July, and September: osmotic potential at full turgor (π_{100}), relative water content at turgor loss point (RWC_{TLP}), water potential at turgor loss point (Ψ_{TLP}), and mean bulk modulus of elasticity (ϵ)

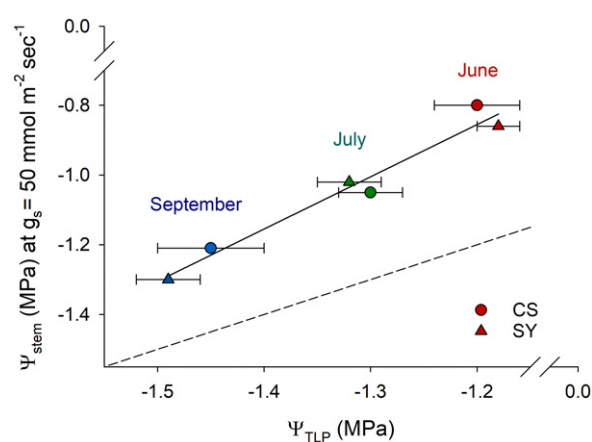
	π_{100} (MPa)	RWC_{TLP} (%)	Ψ_{TLP} (MPa)	ϵ (MPa)
Syrah				
June	-0.94 ± 0.05 a	92.8 ± 0.2	-1.18 ± 0.02 a	11.65 ± 0.68
July	-1.07 ± 0.04 b	89.9 ± 5.0	-1.32 ± 0.03 b	8.14 ± 1.09
September	-1.24 ± 0.04 c	89.7 ± 7.9	-1.49 ± 0.03 c	10.01 ± 1.62
	**	NS	**	NS
Cabernet S.				
June	-0.99 ± 0.05 a	91.0 ± 0.6	-1.20 ± 0.06 a	10.56 ± 0.35
July	-1.08 ± 0.04 b	90.0 ± 0.8	-1.30 ± 0.03 b	9.88 ± 0.88
September	-1.19 ± 0.04 c	90.6 ± 1.2	-1.45 ± 0.05 c	9.11 ± 1.60
	*	NS	*	NS

Values are mean \pm SEM ($n = 6$). * and **Significance at $P < 0.05$ and $P < 0.01$, respectively. NS, not significant ($P > 0.05$). Different letters indicate statistical differences tested after Tukey HSD post-hoc ($P < 0.05$).

**Figure 3.** Stomatal conductance (g_s) response to stem water potential (Ψ_{stem}) during the three different drought experiments (in June, July, and September).

(a) Cabernet Sauvignon and (b) Syrah. Data were fit using a LOESS function. Shadows represent the confidence interval. The same dataset was used for statistical analyses (Figure S4).

significant ($P < 0.05$), Month was significant in Cabernet but not in Syrah, probably because of the higher variability of the g_s data in June and July. However, in both cultivars the significant interaction ($P < 0.05$) among factors

**Figure 4.** Relationship between the turgor loss point (Ψ_{TLP}) and the stem water potential (Ψ_{stem}) at which stomatal conductance (g_s) reaches $50 \text{ mmol m}^{-2} \text{ sec}^{-1}$ (calculated from the exponential regression presented in Figure S4) in Cabernet Sauvignon (circles) and Syrah (triangles) at June (red), July (green), and September (blue). Solid line represents a linear regression using all the points together. Dashed line is the 1:1 curve.

($\Psi_{stem} \times \text{Month}$) indicate that the $g_s \sim \Psi_{stem}$ correlation changed along the season (Figure S4) and therefore the g_s response to Ψ_{stem} was dependent on the moment drought was imposed.

Surprisingly, the $g_s \sim \Psi_{stem}$ curve exhibited a greater change as compared with the Ψ_{TLP} : in Cabernet Sauvignon, the Ψ_{stem} at which $g_s = 50 \text{ mmol m}^{-2} \text{ sec}^{-1}$ (according to the exponential fitting; Figure S4, Table S2) was -0.80 , -1.05 , and -1.21 MPa in June, July, and September, respectively, while in Syrah it was -0.86 , -1.02 , and -1.30 MPa in June, July, and September, respectively (Figure 4).

Modelling

Given the seasonal modifications in π_{100} and Ψ_{TLP} observed in the dehydration experiment, i.e. results in agreement

and within the range of what has been reported in previous studies on grapevines (Alsina et al., 2007; Martorell et al., 2015; Sorek et al., 2021), we integrated a seasonally dynamic cell osmotic concentration (π_{100}) into the SurEau model (Cochard et al., 2021).

The first goal of the simulation was to examine the link between osmotic adjustment and the seasonal trend of $g_s \sim \Psi_{\text{stem}}$ observed in our experiment. The results (Figure S5) confirmed that osmotic accumulation alone is sufficient for shifting the $g_s \sim \Psi_{\text{stem}}$ in a similar manner to those observed in the experiment. Accordingly, dynamic π_{100} was used to explore the effect of the seasonal shift in $g_s \sim \Psi$ under various conditions. For comparison, we also ran the model for a constant π_{100} case (i.e. no osmoregulation during the season).

When modelled without precipitation for 120 days (the typical time period between flowering and harvest in grapevine), the vine with a dynamic π_{100} exhibited an increase of g_s from 218 to 267 $\text{mmol m}^{-2} \text{sec}^{-1}$ during the first part of the soil dehydration (DOY 140–180) and was able to dry the soil to lower Ψ_{soil} of -0.49 MPa as compared with -0.39 MPa in the constant π_{100} vine (Figure 5a,

b). Put another way, the dynamic π_{100} enabled the vines to utilize a higher proportion of the soil water content. However, due to the nature of the soil water retention curve (Figure S6), these lower Ψ_{soil} only added 19 L to the seasonal transpiration of the vine (705 L versus 686 L for the dynamic versus constant π_{100}). Moreover, the higher transpiration rates of the dynamic π_{100} dried the soil faster, reaching critical values of $g_s \leq 50$ $\text{mmol m}^{-2} \text{sec}^{-1}$ (Medrano et al., 2002) after 64 days as compared with 69 days in the constant π_{100} vine (Figure 5b).

When considering the vines' performance with irrigation or rain events (Figure 5c), the differences between dynamic and constant π_{100} become clear. As π_{100} gradually becomes more negative, it allows for a higher g_s , which peaks at 369 $\text{mmol m}^{-2} \text{sec}^{-1}$ at the end of the season as compared with a constant 218 $\text{mmol m}^{-2} \text{sec}^{-1}$ in the constant π_{100} . It is important to mention that all of the above simulations (Figure 5a–c) were conducted under constant climatic conditions (a sigmoidal function of 25°C and 50% relative humidity (RH) at midday and 15°C and 90% RH at pre-dawn). The advantage of the dynamic π_{100} becomes even more evident if we account for the seasonal increases in

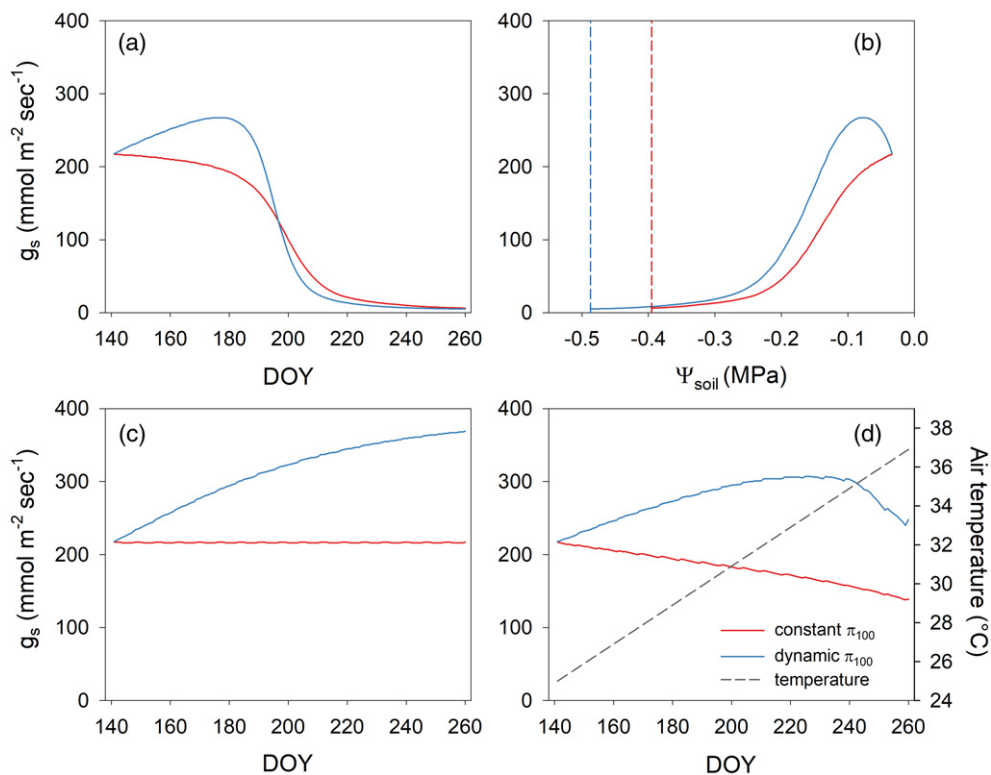


Figure 5. SurEau model outputs of daily maximum stomatal conductance (g_s) considering osmoregulation (dynamic π_{100} ; blue) versus constant π_{100} (red) while simulating different scenarios.

(a) Soil dehydration under constant climate (15/25°C and relative humidity 50/90% for night/day) in respect to time [days of the year (DOY)], or (b) in respect to the soil water potential (Ψ_{soil} ; vertical dashed lines indicate the minimum Ψ_{soil} reached after 120 days simulation); (c) weekly precipitation of 16 mm with the same climatic conditions as in (a), or (d) considering a progressive increase in the daily maximum temperatures of $0.1^\circ\text{C day}^{-1}$ (dashed line) while maintaining a constant vapor content.

temperature between spring and summer (Figure 5d). When we simulated the same monthly watering scenario described for Figure 5c, but increased temperature from 15–25°C to 27–37°C (daily min–max temperature) at a rate of 0.1°C day⁻¹ (this increase corresponds to the maximal VPD doubling from 1.59 to 3.13 kPa), the dynamic π_{100} increased the g_s up to 307 mmol m⁻² sec⁻¹ at DOY 232 while at the same time the constant π_{100} resulted in a considerable reduction of g_s (from 218 to 164 mmol m⁻² sec⁻¹).

Exploring the advantage of a dynamic π_{100} with respect to the past and future climate of Bordeaux also showed that dynamic π_{100} increased the average maximal stomatal conductance by approximately 55 mmol m⁻² sec⁻¹ during the last 70 years (Figure 6). However, the advantage is expected to decrease in the projected future (Figure S7) to <20 mmol m⁻² sec⁻¹ if the average daily max temperature will surpass 30°C and the dryness index (difference between precipitation and ET₀) will be lower than -4 mm.

DISCUSSION

Our results demonstrate that grapevines modify their stomatal regulation during the season in coordination with the adjustment of Ψ_{TLF} to more negative values (Figure 4). The complementary shift of the $g_s \sim \Psi_{\text{stem}}$ curve and the Ψ_{TLF} enabled the vines to maintain gas exchange under lower Ψ_{stem} while avoiding turgor loss. Such characteristics are likely advantageous for deciduous Mediterranean species that start the growing season when water is abundant and the climate is mild but have to continue functioning under hotter and dryer conditions as summer progresses.

Prevalence and drivers of the seasonal plasticity of

$g_s \sim \Psi_{\text{stem}}$

While this study focused on one species only, the seasonal accumulation of osmolytes (presumably contributing to the corresponding shift in Ψ_{TLF}) is common to most grapevine cultivars (Alsina et al., 2007; Düring, 1984; Hochberg et al., 2017a; Martorell et al., 2015; Patakas and Noitsakis, 2001; Sorek et al., 2021), and many other species (Bartlett et al., 2014; Hinckley et al., 1980; Loveys et al., 1987; Parker et al., 1982; Tyree et al., 1978). When combined with the high coordination between Ψ_{TLF} and stomatal closure, this implies that the seasonal shift of the stomatal response curve presented in this paper is not unique to grapevines.

The seasonal changes in leaf hydraulic traits observed here (i.e. stomatal regulation, osmotic adjustment) probably were not driven by external signals, as most environmental parameters (i.e. soil water content or atmospheric conditions) did not coincide with these changes (July was the hottest and driest). In addition, the dependency of Ψ_{TLF} and even stomatal regulation on leaf age (Patakas and Noitsakis, 2001; Patakas et al., 1997) further supports the idea that development may be the primary driver of the

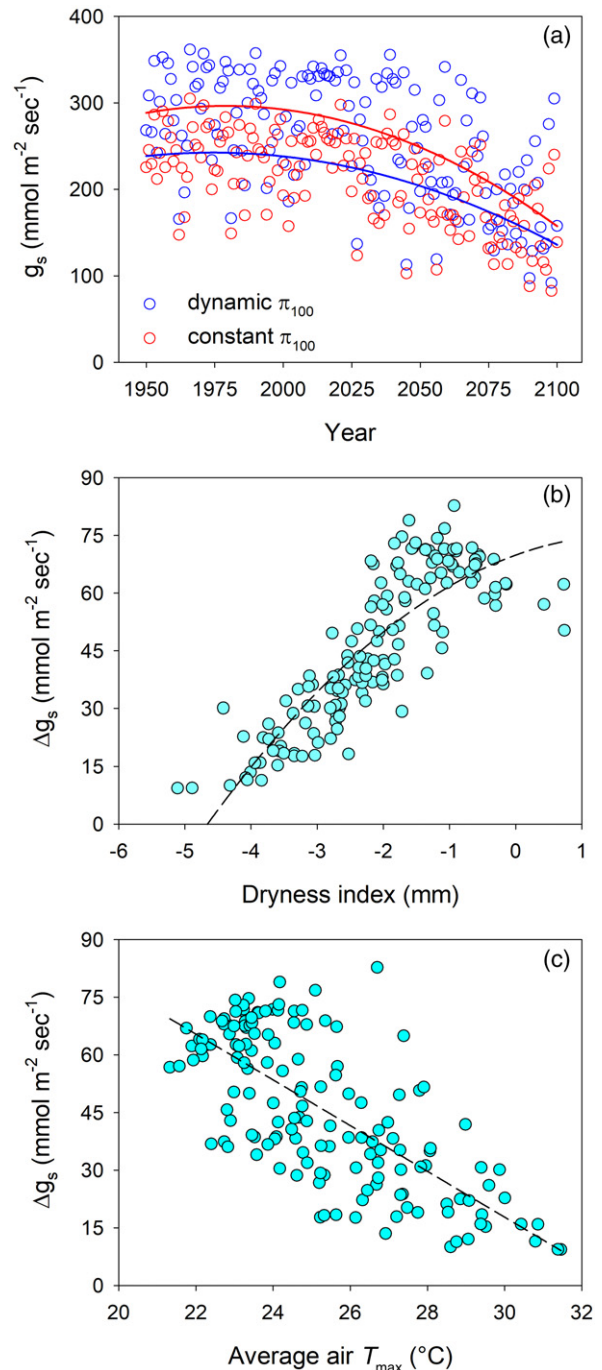


Figure 6. SurEau long-term model output using Bordeaux RCP8.5 simulation data for the years 1950–2100.

The model was limited to the same portion of the growing season used in Figure 5 (DOY = 140–260) and considered vines with or without a dynamic π_{100} of 0.007 MPa day⁻¹.

(a) Yearly average maximum stomatal conductance.

(b) Difference between the yearly average maximum stomatal conductance of the dynamic π_{100} minus the constant π_{100} (Δg_s) in response to seasonal dryness index (calculated as the mean daily difference between precipitation and ET₀ during day of year 140–260).

(c) Δg_s in response to the average maximum air temperature during day of year 140–260.

measured plasticity. Notwithstanding, the experimental design was insufficient to rule out the possibility that the cumulative effect of environmental factors rather than age could signal the observed plasticity.

The coordination between the $g_s \sim \Psi_{\text{stem}}$ and Ψ_{TLP} is expected based on the mechanical link between the turgor and stomatal opening (Edwards and Meidner, 1975), and has been observed for several species (Rodríguez-Domínguez et al., 2016), including grapevines (Dayer et al., 2020). The model results (Figure S5) further show that a change in the leaf osmotic concentration will drive an equal change in $g_s \sim \Psi_{\text{stem}}$. Furthermore, chemical signals for stomatal closure [i.e. abscisic acid (ABA)] were shown to accumulate gradually in leaves that were dried to their Ψ_{TLP} (McAdam and Brodribb, 2016; Pierce and Raschke, 1980). Accordingly, an adjustment of Ψ_{TLP} to lower Ψ_{stem} could be coordinated with, and even partially result from, the adjustment of the hydraulic and chemical signals controlling stomatal closure. In support, Cardoso et al. (2020) showed that drought acclimated sunflowers adjusted their Ψ_{TLP} by 0.33 MPa, leading to a similar shift of the Ψ_{leaf} that leads to ABA accumulation and stomatal closure. However, in the current study, the seasonal adjustment in Ψ_{TLP} (approximately 0.3 MPa) drove an even higher seasonal adjustment of the Ψ_{stem} leading to $g_s = 50 \text{ mmol m}^{-2} \text{ sec}^{-1}$ (approximately 0.6 MPa). One possible explanation for the discrepancy is that the drought event itself affects the adjustment of Ψ_{TLP} (Hochberg et al., 2017a) and that the magnitude of such an adjustment is proportional to the initial Ψ_{TLP} (Bartlett et al., 2016). Therefore, as Ψ_{TLP} was assessed before the drought episodes, it may be overestimated (i.e. less negative than it would be at the corresponding stomatal closure point). In this case, the differences in the plasticity of the two parameters are smaller than the differences portrayed by our results. In addition, other factors that affect stomatal opening, such as stomatal sensitivity to ABA (Tardieu et al., 1993) or cell wall elasticity (Franks et al., 1995), could also be seasonally plastic, meaning that Ψ_{TLP} adjustment alone does not encapsulate the entire seasonal plasticity of the stomata.

Modelling transpiration for exploring the advantages of a dynamic $g_s \sim \Psi_{\text{stem}}$

To explore the consequences of a dynamic stomatal response curve, we used the SurEau hydraulic model, with or without a seasonally dynamic cell osmotic concentration (π_{100}). The model outcomes illustrate how a dynamic π_{100} could result in an increase of g_s during the first few weeks of the season, even if the soil water content is decreasing. As long as the decrease in π_{100} is faster than the decrease in Ψ_{soil} , g_s should increase. Such conditions are expected for irrigated trees, but also for trees with access to a substantial soil water reservoir early in the season. Owing to the nature of the soil retention curve, the

first part of soil dehydration does not have a significant effect on Ψ_{soil} . The early season increase in transpiration under our theoretical framework has actually been observed in many deciduous species such as red oaks (Gersony et al., 2020), grapevines (Sorek et al., 2021; Torres et al., 2021), and others (Novak et al., 2005; Prior et al., 1997; Xu and Baldocchi, 2003). This agreement between the model results and field measurements highlights the importance of integrating the dynamic stomatal response curve into our basic principles of plant hydraulics.

Because the accumulation of osmolytes for stomatal opening under lower Ψ_{stem} has an energetic cost (Turner and Begg, 1981), we could assume that the seasonal reduction in π_{100} should offer the vines an advantage. Furthermore, the fact that most plants accumulate osmolytes in response to stress (Bartlett et al., 2014; Hochberg et al., 2017a) suggests that the seasonal osmotic adjustment has an advantage under drought conditions. It is clear that lower π_{100} should allow the vines to maintain gas exchange under lower Ψ_{stem} , but the overall advantage of such behaviour is not straightforward.

It seems logical that lower π_{100} should enable the vines to utilize a larger proportion of the soil water content under a long drought. At the same time, our model simulation showed that under a season-long drought (120 days), a dynamic π_{100} would have only a marginal contribution to the soil extractable water (approximately 2.5%) (Figure 5b). Similar conclusions were drawn from a model of Sinclair and Muchow (2001) that simulated the effect of delayed stomatal closure due to osmotic adjustment. It is possible that differently from our (or Sinclair and Muchow, 2001) simulations where root volume was fixed, the root volume actually increases under drought conditions (Chaudhuri et al., 1990; Hsiao and Xu, 2000; Pace et al., 1999; Zhang et al., 2016), and in combination with a higher driving force (lower Ψ_{stem}), could result in a significant increase of the soil extractable water. In fact, Serraj and Sinclair (2002) have speculated that the importance of osmotic adjustment lies in its ability to promote root growth under water stress. Specifically in grapevines, measurements of a seasonal increase in the whole root system conductance (Alsina et al., 2011) imply that a seasonal increase in rooting volume is possible, but more data are required before we can understand its relevance (Gambetta et al., 2020).

The advantage of a dynamic π_{100} seems to be much more prominent when water is available. A dynamic π_{100} should enable the vines to maintain higher g_s (which are coupled to higher CO_2 assimilation rates) (Figure 5c). The differences between the dynamic versus constant π_{100} are even clearer when irrigation/precipitation is simulated (Figure 5d). Under mild drought conditions, vines with a dynamic π_{100} should be able to increase their g_s , while vines with a constant π_{100} downregulate g_s . Finally, when considering the typical variation in VPD between spring

and the summer peak, the advantage becomes clearer. With a constant π_{100} , a vine would need to lower its g_s as summer progresses and the VPD increases. A seasonal coordination of π_{100} with the atmospheric conditions is required for the optimization of the leaf economy (achieving higher CO_2 assimilation rates under periods of stress), and such behaviour would be in agreement with previously reported stomatal responses observed in other Mediterranean deciduous species (Mediavilla and Escudero, 2003).

Future perspective and implications

The magnitude, timing, and direction of the shifts in stomatal response described in this work have striking parallels to the seasonal plasticity of stem (Charrier et al., 2018) and leaf (Martorell et al., 2015; Sorek et al., 2021) vulnerability to embolism. Therefore, grapevines appear to exhibit a coordinated increase in drought tolerance as the season progresses across multiple traits and even organs.

These observations have important implications for future studies. First, extrapolating conclusions from fast-drying pot experiments (which normally impose water stress in 5–10 days, such as the case here) to the field setting could be misleading. For example, several pot studies reported near minimal g_s when grapevines were dried to Ψ_{stem} of -1 MPa (e.g. Hochberg et al., 2017a). In contrast, nearly all field studies reported substantial gas exchange ($g_s > 50 \text{ mmol m}^{-2} \text{ sec}^{-1}$) even under lower Ψ_{stem} (e.g. Munitz et al., 2020). Similar differences between potted and field vines were reported in Charrier et al. (2018). This apparent contradiction arises from the fact that under field conditions, Ψ_{stem} lower than -1 MPa rarely develops before July (Charrier et al., 2018; Herrera et al., 2015; Intrigliolo and Castel, 2008; Martorell et al., 2015; Savi et al., 2019), and by that time, the g_s - Ψ_{stem} curve has already shifted. This suggests that attempting to integrate leaf level hydraulic data across studies without controlling for the developmental effect could be erroneous.

Furthermore, we believe that the attention that grapevine research has dedicated to the differences in stomatal regulation between varieties (e.g. Hochberg et al., 2013; Schultz, 2003) should consider the seasonal plasticity. In the current study, the effects of seasonality on stomatal regulation were significantly larger than the varietal effect. In fact, the two varieties studied here did not actually exhibit different stomatal response curves despite previous reports of such differences between Syrah and Cabernet Sauvignon (Hochberg et al., 2013; Tramontini et al., 2014). Even in those studies that did find significant differences between these varieties, they were rarely as substantial as the seasonal differences presented in this study. Dayer et al. (2020) showed an approximate 0.4 MPa difference between different grapevine varieties in their stomatal closure threshold, which is similar in magnitude to the

seasonal shifts shown in this study. This stresses the importance of focusing future studies on the seasonal dynamics of physiological traits, which could be as great, or greater [approximately 1 MPa in Alsina et al. (2007) and Sorek et al., (2021)], than innate genetic differences. In fact, differences in developmental rates or osmolyte accumulation rates between cultivars could be part of the source for the reported variability in stomatal regulation (Schultz, 2003). Taking these seasonal changes into account could improve our understanding of drought acclimation and irrigation requirements.

Finally, it seems that under current climate conditions, osmotic adjustment and its effect on the g_s - Ψ_{stem} enables plants to increase g_s , probably leading to higher productivity (Figure 6a). However, as the benefit of the dynamic g_s - Ψ_{stem} mostly manifests under mild water deficits, projected warmer scenarios associated with climate change (leading to an increase in the aridity gradient) is likely to reduce its advantage (Figure 6b,c). Furthermore, the fact that the thresholds for stomatal closure are at quite a high Ψ_{stem} early in the season raise concerns that an increase in the frequency of early-season drought events could have a disproportionately negative impact on productivity and even survival.

In conclusion, this study provides evidence for a seasonal shift of grapevine's stomatal response curve in coordination with the adjustment of Ψ_{TLP} . Such dynamics explain the early season increase in transpiration and improve the vines' ability to maintain gas exchange under higher VPD and water deficit. Integrating the seasonal stomatal plasticity into current models should improve our ability to predict plant water requirements and more accurately assess the risks associated with future climate change.

EXPERIMENTAL PROCEDURES

Dehydration experiment

Plant material and experimental site. The experiment was carried out at the experimental farm of the University of Udine 'A. Servadei', located in the Friuli Venezia Giulia region (NorthEastern Italy; $46^{\circ}02' \text{ N}$, $13^{\circ}13' \text{ E}$; 88 m a.s.l.). In total, 150 vines of *Vitis vinifera* cv. Cabernet Sauvignon (clone R5) and 150 vines of *Vitis vinifera* L. cv. Syrah (clone ISV-R1), both grafted on SO4 rootstock, were acquired from VCR nursery (certified plant material) and planted on 15 April 2016 in 7-L white plastic pots. Pots were filled with sieved soil supplemented with 20% perlite as described in Hochberg et al. (2017b). To prevent rain from influencing the trials, the vines were grown under a 4.5-m high tunnel opened on the sides and roofed with a clear plastic film (ethylene-vinyl-acetate; Patilux, Treviso, Italy) as described in Herrera et al. (2015). The plants were organized in two rows, and one single shoot per plant was retained and trained vertically. When the shoot length exceeded the height of the trellising system (2.1 m) the shoot was positioned horizontally in the last catching wire. Budbreak, stage E-L 4 (Coombe, 1995), occurred on 5 May (DOY 125) in both cultivars. Water was supplied by a pressure-compensated drip

irrigation system with one emitter per pot (PCJ 2 L h⁻¹; Netafim, Hatzetim, Israel) using the system described in (Hochberg et al., 2017b). All vines were irrigated twice a day (at 14.00 and at 23.00 h) to saturation (approximately 2.3 L day⁻¹) until the imposition of drought conditions.

Treatments and monitoring. During the experimental phase, four treatments were imposed: well-watered (WW), June water-stressed (WS), July WS, and September WS. In WW, irrigation was maintained as described above during the whole season. WS was imposed in three different dates during the season: 21 June (DOY 172), 18 July (DOY 199), and 12 September (DOY 255), and always on different plants (i.e. at each date, a group of 30 homogeneous vines was selected and subjected to WS; each group of drought-stressed vines was therefore stressed only once and was not further considered for the successive experiments). WS was imposed by withholding irrigation (removing the dripper from the pot) until reaching visible signs of dehydration, such as leaf wilting and abscission (approximately 10 days). Leaf area was assessed before the beginning of each trial to ensure a similar plant size among the treatments. Leaf area was calculated by measuring the main vein (midrib) length of all the leaves in the shoots and using a regression between leaf length and leaf area that was constructed with 50 different leaves per cultivar ($R^2 = 0.97$ and 0.98 for Cabernet and Syrah, respectively) using a leaf area meter (LI-3100C; LiCor, Inc., Lincoln, NE, USA).

Ψ_{stem} and g_s were measured at midday (between 11.00 and 14.00 h) every day during the periods of water stress, except on cloudy days. For the determination of Ψ_{stem} , fully expanded leaves were bagged and covered with aluminium foil 30 min before the measurement and then excised with a razor blade. Thereafter, the leaves were placed in a Scholander pressure bomb (Soil Moisture Co., Santa Barbara, CA, USA) with the petiole protruding from the chamber and pressurized using nitrogen. At each sampling date, one leaf per vine from three different vines per treatment was used for Ψ_{stem} measurements. g_s was measured in sun-exposed and fully developed leaves (one leaf per vine from nine different vines per treatment) with a portable photosynthesis system LI-6400 XT (LiCor, Inc.), using a constant light intensity (1000 $\mu\text{mol m}^{-2} \text{sec}^{-1}$), CO_2 concentration (400 $\mu\text{mol mol}^{-1}$), and ambient temperature and humidity.

Finally, on the day of every WS imposition, a set of leaves from five different vines per cultivar were sampled in the early morning for the construction of pressure–volume curves (PV). To assure full hydration, the petiole was submerged in water for 4 h under dark conditions. From each vine, two leaves were collected, one from the seventh and one from the 12th node (counted positions from the base of the shoot). PV curves were obtained using the bench dry method, where leaf weight and leaf water potential (Ψ_l) are periodically measured while progressively drying leaves on a laboratory bench. From the PV curves, Ψ_l at the turgor loss point (Ψ_{TLP}), osmotic potential at full turgor (π_{100}), and modulus of elasticity (ϵ) were calculated according to Bartlett et al. (2012).

Statistical analyses

Data were analysed using SPSS version 26.0 (IBM Corp., Armonk, NY, USA). ANOVA was used to identify differences between treatments (the period of WS imposition) in leaf traits calculated from the PV curves and post-hoc Tukey's honestly significant difference tests used to separate means; in all cases $P < 0.05$ was used for significance. The $g_s \sim \Psi_{\text{stem}}$ curves were fitted using a LOESS regression with the ggplot2 package in R (Wickham, 2016) with confidence intervals (95%) to visualize differences between

periods of WS imposition. Furthermore, to transform the $g_s \sim \Psi_{\text{stem}}$ curve into a single value that could be compared with the Ψ_{TLP} , the same dataset was used to fit exponential curves and calculate the Ψ_{stem} at which $g_s = 50 \text{ mmol m}^{-2} \text{sec}^{-1}$ (Table S2), a marker for severe drought in stress in grapevines, which subject plants to non-stomatal limitation to photosynthesis (Medrano et al., 2002). We did not calculate the Ψ_{stem} , which leads to g_s values that are more typical for vines at Ψ_{TLP} (approximately $10 \text{ mmol m}^{-2} \text{sec}^{-1}$) because of the uncertainty in the model when g_s aspires to 0. To test differences between the $g_s \sim \Psi_{\text{stem}}$ curves obtained from the three drought experiments, we calculated the model $g_s \sim \Psi_{\text{stem}}$ using R, so that significant interactions explain that the $g_s \sim \Psi_{\text{stem}}$ correlation changed among experiments (Figure S4).

Modelling the effect of seasonal dynamic stomatal closure

To highlight the outcomes of a seasonally dynamic $g_s \sim \Psi$, we used a mechanistic soil–plant water transport model (SurEau; Cochard et al., 2021). Based on our results and other findings of a seasonal adjustment of the turgor loss (Alsina et al., 2007; Martorell et al., 2015; Sorek et al., 2021), we integrated a seasonally dynamic cell osmotic concentration (π_{100}) into the model, expecting it to drive a seasonal shift in $g_s \sim \Psi$.

The first goal was to see if the model can capture the link between osmotic adjustment (as π_{100} dynamic) and the seasonal trend of $g_s \sim \Psi_{\text{stem}}$ observed in our pot experiment. We set all conditions to match our experiment. Pot volume was set to 7 L filled with loamy soil ($\theta_s = 0.396$; $\theta_r = 0.131$; $\alpha = 0.00423$; $m = 0.51456$; $n = 2.06$; taken from van Genuchten, 1980). Leaf area, π_{100} , ϵ , and climatic conditions were set to observed values at the three dates (Table 1 and Table S1). The branch diameter was set to 1 cm in June and increased in July and September to maintain a constant Huber value. The whole tree leaf-area specific conductance ($5.5 \text{ mmol sec}^{-1} \text{MPa}^{-1} \text{m}^{-2}$) was calculated to match the observed transpiration rates and water potentials of WW plants. Within the plant, conductance was divided equally between leaves (1/3), shoots (1/3), and the root system (1/3). To derive the $g_s \sim \Psi$ relationship, we fitted a sigmoid response curve of g_s between αP_{100} and turgor loss ($P = 0$), with P_{100} the leaf turgor at full hydration and α an empirical parameter set to 0.6. All other parameters were identical to Cochard et al. (2021).

Recognizing that a dynamic π_{100} will drive an equal dynamics of $g_s \sim \Psi$, our second goal was to explore the potential advantages of seasonal changes in $g_s \sim \Psi$ on a more realistic scenario using average field-size plants in a vineyard. We simulated vines with a canopy area of 5 m² at a planting density of 3 × 1.5 m, resulting in a leaf area index of 1.1. We assumed a 1.5-m rooting depth, leading to a 6.8-m³ rooting volume and 754 L between field capacity and the residual water content. Other soil and plant characteristics were set as described above. To avoid complications with the dynamics of root and canopy development, we assumed that the canopy and root system were fully developed already at DOY 140. To simulate a gradual osmotic adjustment, we defined π_{100} as -0.8 MPa in DOY 140 (a bit higher than what we measured in June; see Results section) and allowed it to decrease at a constant rate of $-0.007 \text{ MPa day}^{-1}$, as was shown by previous studies for Ψ_{TLP} seasonal dynamics (Alsina et al., 2007; Martorell et al., 2015; Sorek et al., 2021). The vines with dynamic π_{100} were compared with similar vines bearing a constant π_{100} of -0.8 MPa under two irrigation regimes (without irrigation or with 16 mm week⁻¹) and two climatic conditions (with constant night/day temperature of 15/25°C and RH of 90/50%; or with a gradual increase of 0.1°C day⁻¹ while maintaining constant vapour concentration).

Finally, to examine the effect of osmotic adjustment on vineyards under natural climatic conditions, we ran the model with the 1950–2020 climate of Bordeaux (Merignac weather station, extracted from the INRAE CLIMATIK platform), assuming no irrigation. To examine the importance of osmotic adjustment under the potentially very hot future, we ran the model with RCP 8.5 (Riahi et al., 2011) until the year 2100. We selected the CNRM-CM5 DRIAS/ALADIN climatic model and extracted daily data from the INRAE SICLIMA platform for grid cell 6473.

The SurEau model is used here as a framework for thought experiments to understand the consequences/importance of Ψ_{TLP} seasonal adjustment.

ACKNOWLEDGEMENTS

The authors thank Mr. Moreno Greatti for his assistance in plant protection. The work was partially supported by the EU, ERA-NET, ARIMNET2 project “Opportunities for an Environmental-friendly Viticulture: EnViRoS” and by the Austrian Science Fund (FWF): I 4848 “PlasticGrape”. Open access funding provided by University of Natural Resources and Life Sciences, Vienna (BOKU).

AUTHOR CONTRIBUTIONS

JCH and UH conceptualized and wrote the original draft. AC, PS, and JCH carried out the experimental part under supervision from EP. UH, JCH, and HC performed the model analysis. AF, GG, EP, and HC critically reviewed the draft. All authors read and approved the manuscript.

CONFLICT OF INTERESTS

The authors declare that they have no competing interests.

DATA AVAILABILITY STATEMENT

All relevant data can be found within the manuscript and its supporting materials. The C code of SurEau v.20-12-26 (Cochard et al., 2021) used for this study is available from the data INRAE public repository: <https://data.inrae.fr/dataset.xhtml?persistentId=doi:10.15454/6Z1MXK>.

SUPPORTING INFORMATION

Additional Supporting Information may be found in the online version of this article.

Figure S1. Meta-analysis of pre-dawn and midday leaf water potential of grapevines.

Figure S2. Climate data during experiments.

Figure S3. Midday stem water potential presented as the difference between WS and WW ($\Delta\Psi_{\text{stem}}$).

Figure S4. $g_s \sim \Psi_{\text{stem}}$ exponential fitting and statistics.

Figure S5. Checking the model's ability to modify the $g_s \sim \Psi_{\text{stem}}$ curve based solely on the shift in the cell osmotic concentration (π_{100}).

Figure S6. Soil moisture release curve of the soil used in the model.

Figure S7. Yearly averages of the daily maximum air temperature ($^{\circ}\text{C}$) and ET_0 at Bordeaux using the RCP8.5 simulation data for the years 1950–2100.

Table S1. Total leaf area and number of leaves measured in the main and lateral shoots.

Table S2. Regression reports from Figure S4.

REFERENCES

- Alsina, M.M., De Herralde, F., Aranda, X., Savé, R. & Biel, C. (2007) Water relations and vulnerability to embolism are not related: experiments with eight grapevine cultivars. *VITIS - Journal of Grapevine Research*, **46**, 1–6.
- Alsina, M.M., Smart, D.R., Bauerle, T., De Herralde, F., Biel, C., Stockert, C. et al. (2011) Seasonal changes of whole root system conductance by a drought-tolerant grape root system. *Journal of Experimental Botany*, **62**, 99–109.
- Bartlett, M.K., Klein, T., Jansen, S., Choat, B. & Sack, L. (2016) The correlations and sequence of plant stomatal, hydraulic, and wilting responses to drought. *Proceedings of the National Academy of Sciences of the United States of America*, **113**, 13098–13103.
- Bartlett, M.K., Scoffoni, C. & Sack, L. (2012) The determinants of leaf turgor loss point and prediction of drought tolerance of species and biomes: a global meta-analysis. *Ecology Letters*, **15**, 393–405.
- Bartlett, M.K., Zhang, Y., Kreidler, N., Sun, S., Ardy, R., Cao, K. et al. (2014) Global analysis of plasticity in turgor loss point, a key drought tolerance trait. *Ecology Letters*, **17**, 1580–1590.
- Brodribb, T.J., Holbrook, N.M., Edwards, E.J. & Gutiérrez, M.V. (2003) Relations between stomatal closure, leaf turgor and xylem vulnerability in eight tropical dry forest trees. *Plant, Cell and Environment*, **26**, 443–450.
- Brown, K.W., Jordan, W.R. & Thomas, J.C. (1976) Water stress induced alterations of the stomatal response to decreases in leaf water potential. *Physiologia Plantarum*, **37**, 1–5.
- Buckley, T.N. (2019) How do stomata respond to water status? *New Phytologist*, **224**, 21–36.
- Cardoso, A.A., Brodribb, T.J., Kane, C.N., DaMatta, F.M. & McAdam, S.A.M. (2020) Osmotic adjustment and hormonal regulation of stomatal responses to vapour pressure deficit in sunflower. *AoB Plants*, **12**.
- Charrier, G., Delzon, S., Domec, J.-C.-J., Zhang, L., Delmas, C.E.L., Merlin, I. et al. (2018) Drought will not leave your glass empty: Low risk of hydraulic failure revealed by long-term drought observations in world's top wine regions. *Science Advances*, **4**, eaao6969.
- Chaudhuri, U.N., Kirkham, M.B. & Kanemasu, E.T. (1990) Root growth of winter wheat under elevated carbon dioxide and drought. *Crop Science*, **30**, 853–857.
- Cochard, H., Pimont, F., Ruffault, J. & Martin-StPaul, N. (2021) SurEau: a mechanistic model of plant water relations under extreme drought. *Annals of Forest Science*, **78**, 55.
- Coombe, B.G. (1995) Growth stages of the grapevine: adoption of a system for identifying grapevine growth stages. *Australian Journal of Grape and Wine Research*, **1**, 104–110.
- Darwin, F. (1898) Observations on stomata. *Philosophical Transactions of the Royal Society of London Series B, Biological Sciences Series B, Containing Papers of a Biological Character*, **190**, 531–621.
- Dayer, S., Herrera, J.C., Dai, Z., Burlett, R., Lamarque, L.J., Delzon, S. et al. (2020) The sequence and thresholds of leaf hydraulic traits underlying grapevine varietal differences in drought tolerance. *Journal of Experimental Botany*, **71**, 4333–4344.
- Düring, H. (1984) Evidence for osmotic adjustment to drought in grapevines (*Vitis vinifera* L.). *Vitis*, **23**, 1–10.
- Edwards, M. & Meidner, H. (1975) Micromanipulation of stomatal guard cells. *Nature*, **253**, 114–115.
- Farrell, C., Szota, C. & Arndt, S.K. (2017) Does the turgor loss point characterize drought response in dryland plants? *Plant, Cell and Environment*, **40**, 1500–1511.
- Field, C.B., Jackson, R.B. & Mooney, H.A. (1995) Stomatal responses to increased CO₂: implications from the plant to the global scale. *Plant, Cell and Environment*, **18**, 1214–1225.
- Franks, P.J., Cowan, I.R., Tyerman, S.D., Cleary, A.L., Lloyd, J. & Farquhar, G.D. (1995) Guard cell pressure/aperture characteristics measured with the pressure probe. *Plant, Cell and Environment*, **18**, 795–800.
- Franks, P.J., Drake, P.L. & Froend, R.H. (2007) Anisohydric but isohydrodynamic: seasonally constant plant water potential gradient explained by a stomatal control mechanism incorporating variable plant hydraulic conductance. *Plant, Cell and Environment*, **30**, 19–30. <https://doi.org/10.1111/j.1365-3040.2006.01600.x>
- Gambetta, G.A., Herrera, J.C., Dayer, S., Feng, Q., Hochberg, U. & Castel-Larin, S.D. (2020) The physiology of drought stress in grapevine: towards an integrative definition of drought tolerance. *Journal of Experimental Botany*, **71**, 4658–4676.

- Gersony, J.T., Hochberg, U., Rockwell, F.E., Park, M., Gauthier, P.P. & Holbrook, N.M. (2020) Leaf carbon export and nonstructural carbohydrates in relation to diurnal water dynamics in mature oak trees. *Plant Physiology*, **183**, 1612–1621.
- Hardie, W.J. & Considine, J.A. (1976) Response of grapes to water-deficit stress in particular stages of development. *American Journal of Enology and Viticulture*, **27**, 55–61.
- Henry, C., John, G.P., Pan, R., Bartlett, M.K., Fletcher, L.R., Scoffoni, C. et al. (2019) A stomatal safety-efficiency trade-off constrains responses to leaf dehydration. *Nature Communications*, **10**, 1–9.
- Herrera, J.C., Bucchetti, B., Sabbatini, P., Comuzzo, P., Zulini, L., Vecchione, A. et al. (2015) Effect of water deficit and severe shoot trimming on the composition of *Vitis vinifera* L. Merlot grapes and wines. *Australian Journal of Grape and Wine Research*, **21**, 254–265.
- Hinckley, T.M., Duhme, F., Hinckley, A.R. & Richter, H. (1980) Water relations of drought hardy shrubs: osmotic potential and stomatal reactivity. *Plant, Cell and Environment*, **3**, 131–140.
- Hochberg, U., Bonel, A.G., David-Schwartz, R., Degu, A., Fait, A., Cochard, H. et al. (2017a) Grapevine acclimation to water deficit: the adjustment of stomatal and hydraulic conductance differs from petiole embolism vulnerability. *Planta*, **245**, 1091–1104.
- Hochberg, U., Degu, A., Fait, A. & Rachmilevitch, S. (2013) Near isohydric grapevine cultivar displays higher photosynthetic efficiency and photorespiration rates under drought stress as compared with near anisohydric grapevine cultivar. *Physiologia Plantarum*, **147**, 443–452.
- Hochberg, U., Herrera, J.C., Degu, A., Castellarin, S.D., Peterlunger, E., Alberti, G. et al. (2017b) Evaporative demand determines the relative transpirational sensitivity of deficit-irrigated grapevines. *Irrigation Science*, **35**, 1–9.
- Hochberg, U., Rockwell, F.E., Holbrook, N.M. & Cochard, H. (2018) Iso/Anisohydry: a plant–environment interaction rather than a simple hydraulic trait. *Trends in Plant Science*, **23**, 112–120.
- Hsiao, T.C., Acevedo, E., Fereres, E. & Henderson, D. (1976) Water stress, growth and osmotic adjustment. *Philosophical Transactions of the Royal Society of London*, **273**, 479–500.
- Hsiao, T.C. & Xu, L.K. (2000) Sensitivity of growth of roots versus leaves to water stress: biophysical analysis and relation to water. *Journal of Experimental Botany*, **51**, 1595–1616.
- Intrigliolo, D.S. & Castel, J.R. (2008) Effects of irrigation on the performance of grapevine cv. Tempranillo in Requena, Spain. *American Journal of Enology and Viticulture*, **59**, 30–38.
- Jasechko, S., Sharp, Z.D., Gibson, J.J., Birks, S.J., Yi, Y. & Fawcett, P.J. (2013) Terrestrial water fluxes dominated by transpiration. *Nature*, **496**, 347–350.
- Jordan, W.R., Brown, K.W. & Thomas, J.C. (1975) Leaf age as a determinant in stomatal control of water loss from cotton during water stress. *Plant Physiology*, **56**, 595–599.
- Klein, T. (2014) The variability of stomatal sensitivity to leaf water potential across tree species indicates a continuum between isohydric and anisohydric behaviours. *Functional Ecology*, **28**, 1313–1320.
- Loveys, B.R., Robinson, S.P. & Downton, W.J.S. (1987) Seasonal and diurnal changes in abscisic acid and water relations of apricot leaves (*Prunus armeniaca* L.). *New Phytologist*, **107**, 15–27.
- Martorell, S., Medrano, H., Tomás, M., Escalona, J.M., Flexas, J. & Diaz-Espejo, A. (2015) Plasticity of vulnerability to leaf hydraulic dysfunction during acclimation to drought in grapevines: an osmotic-mediated process. *Physiologia Plantarum*, **153**, 381–391.
- McAdam, S.A.M. & Brodribb, T.J. (2016) Linking turgor with ABA biosynthesis: implications for stomatal responses to vapor pressure deficit across land plants. *Plant Physiology*, **171**, 2008–2016.
- Mediavilla, S. & Escudero, A. (2003) Stomatal responses to drought at a Mediterranean site: a comparative study of co-occurring woody species differing in leaf longevity. *Tree Physiology*, **23**, 987–996.
- Medrano, H., Escalona, J.M., Bota, J., Gulías, J. & Flexas, J. (2002) Regulation of photosynthesis of C3 plants in response to progressive drought: stomatal conductance as a reference parameter. *Annals of Botany*, **89**, 895–905.
- Meidner, H. & Edwards, M. (1975) Direct measurements of turgor pressure potentials of guard cells. I. *Journal of Experimental Botany*, **26**, 319–330.
- Morison, J.I.L. (2001) Increasing atmospheric CO₂ and stomata. *New Phytologist*, **149**, 154–156.
- Munitz, S., Schwartz, A. & Netzer, Y. (2020) Effect of timing of irrigation initiation on vegetative growth, physiology and yield parameters in Cabernet Sauvignon grapevines. *Australian Journal of Grape and Wine Research*, **26**, 220–232.
- Naor, A. (2008) Water stress assessment for irrigation scheduling of deciduous trees. *Acta Horticulture*, **792**, 467–481.
- Naor, A., Schneider, D., Ben-Gal, A., Zipori, I., Dag, A., Kerem, Z. et al. (2013) The effects of crop load and irrigation rate in the oil accumulation stage on oil yield and water relations of ‘Koroneiki’ olives. *Irrigation Science*, **31**, 781–791.
- Novak, K., Schaub, M., Fuhrer, J., Skelly, J.M., Hug, C., Landolt, W. et al. (2005) Seasonal trends in reduced leaf gas exchange and ozone-induced foliar injury in three ozone sensitive woody plant species. *Environmental Pollution*, **136**, 33–45.
- O’Toole, J.C. & Cruz, R.T. (1980) Response of leaf water potential, stomatal resistance, and leaf rolling to water stress. *Plant Physiology*, **65**, 428–432.
- Pace, P.F., Cralle, H.T., El-Halawany, S.H.M., Cothren, J.T. & Senseman, S.A. (1999) Drought-induced changes in shoot and root growth of young cotton plants. *Journal of Cotton Science*, **3**, 183–187.
- Padgett-Johnson, M., Williams, L.E. & Walker, M.A. (2003) Vine water relations, gas exchange, and vegetative growth of seventeen *Vitis* species grown under irrigated and nonirrigated conditions in California. *Journal of the American Society for Horticultural Science*, **128**, 269–276.
- Parker, W.C., Pallardy, S.G., Hinckley, T.M. & Teskey, R.O. (1982) Seasonal changes in tissue water relations of three woody species of the *Quercus-Carya* forest type. *Ecology*, **63**, 1259–1267.
- Patakas, A. & Noitsakis, B. (2001) Leaf age effects on solute accumulation in water-stressed grapevines. *Journal of Plant Physiology*, **158**, 63–69.
- Patakas, A., Noitsakis, B. & Stavrakas, D. (1997) Adaptation of leaves of *Vitis vinifera* L. to seasonal drought as affected by leaf age. *Vitis*, **36**, 11–14.
- Pierce, M. & Raschke, K. (1980) Correlation between loss of turgor and accumulation of abscisic acid in detached leaves. *Planta*, **148**, 174–182.
- Prior, L.D., Eamus, D. & Duff, G.A. (1997) Seasonal trends in carbon assimilation, stomatal conductance, pre-dawn leaf water potential and growth in *Terminalia ferdinandiana*, a deciduous tree of northern Australian savannas. *Australian Journal of Botany*, **45**, 53–69.
- Radin, J.W. (1984) Stomatal responses to water stress and to abscisic acid in phosphorus-deficient cotton plants. *Plant Physiology*, **76**, 392–394.
- Radin, J.W. & Ackerson, R.C. (1981) Water relations of cotton plants under nitrogen deficiency. *Plant Physiology*, **67**, 115–119.
- Riahi, K., Rao, S., Krey, V., Cho, C., Chirkov, V., Fischer, G. et al. (2011) RCP 8.5-A scenario of comparatively high greenhouse gas emissions. *Climatic Change*, **109**, 33–57.
- Rodriguez-Dominguez, C.M., Buckley, T.N., Egea, G., de Cires, A., Hernandez-Santana, V., Martorell, S. et al. (2016) Most stomatal closure in woody species under moderate drought can be explained by stomatal responses to leaf turgor. *Plant, Cell and Environment*, **39**, 2014–2026.
- Savi, T., Petruzzellis, F., Moretti, E., Stenni, B., Zini, L., Martellos, S. et al. (2019) Grapevine water relations and rooting depth in karstic soils. *Science of the Total Environment*, **692**, 669–675.
- Schultz, H.R. (2003) Differences in hydraulic architecture account for near-isohydric and anisohydric behaviour of two field-grown *Vitis vinifera* L. cultivars during drought. *Plant, Cell and Environment*, **26**, 1393–1405.
- Sepúlveda, G. & Kliewer, W.M. (1986) Stomatal response of three grapevine cultivars (*Vitis vinifera* L.) to high temperature. *American Journal of Enology and Viticulture*, **37**, 44–52.
- Serraj, R. & Sinclair, T.R. (2002) Osmolyte accumulation: can it really help increase crop yield under drought conditions? *Plant, Cell and Environment*, **25**, 333–341.
- Sinclair, T.R. & Muchow, R.C. (2001) System analysis of plant traits to increase grain yield on limited water supplies. *Agronomy Journal*, **93**, 263–270.
- Sorek, Y., Greenstein, S., Netzer, Y., Shtein, I., Jansen, S. & Hochberg, U. (2021) An increase in xylem embolism resistance of grapevine leaves during the growing season is coordinated with stomatal regulation, turgor loss point, and intervessel pit membranes. *New Phytologist*, **229**, 1955–1969.
- Tardieu, F., Zhang, J. & Gowing, D.J.G. (1993) Stomatal control by both [ABA] in the xylem sap and leaf water status: a test of a model for droughted or ABA-fed field-grown maize. *Plant, Cell and Environment*, **16**, 413–420.

- Torres, N., Yu, R., Martínez-Lüscher, J., Kostaki, E. & Kurtural, S.K.** (2021) Application of fractions of crop evapotranspiration affects carbon partitioning of grapevine differentially in a hot climate. *Frontiers in Plant Science*, **12**, 75.
- Tramontini, S., Döring, J., Vitali, M., Ferrandino, A., Stoll, M. & Lovisolo, C.** (2014) Soil water-holding capacity mediates hydraulic and hormonal signals of near-isohydric and near-anisohydric *Vitis* cultivars in potted grapevines. *Functional Plant Biology*, **41**, 1119–1128.
- Turner, N.C. & Begg, J.E.** (1981) Plant-water relations and adaptation to stress. *Plant and Soil*, **58**, 97–131.
- Tyree, M.T., Cheung, Y.N.S., MacGregor, M.E. & Talbot, A.J.B.** (1978) The characteristics of seasonal and ontogenetic changes in the tissue – water relations of *Acer*, *Populus*, *Tsuga*, and *Picea*. *Canadian Journal of Botany*, **56**, 635–647.
- van Genuchten, M.T.** (1980) A closed-form equation for predicting the hydraulic conductivity of unsaturated soils. *Soil Science Society of America Journal*, **44**, 892–898.
- Wickham, H.** (2016) *Ggplot2: elegant graphics for data analysis*, 2nd edn. New York, NY: Springer.
- Xu, L. & Baldocchi, D.D.** (2003) Seasonal trends in photosynthetic parameters and stomatal conductance of blue oak (*Quercus douglasii*) under prolonged summer drought and high temperature. *Tree Physiology*, **23**, 865–877.
- Zhang, L., Marguerit, E., Rossdeutsch, L., Ollat, N. & Gambetta, G.A.** (2016) The influence of grapevine rootstocks on scion growth and drought resistance. *Theoretical and Experimental Plant Physiology*, **28**, 143–157.